Mechanism of inhibition of connexin channels by the quinine derivative *N*-benzylquininium

Clio Rubinos,[1] Helmuth A. Sánchez,[2] Vytas K. Verselis,[2] and Miduturu Srinivas[1]

[1]Department of Biological Sciences, SUNY College of Optometry, New York, NY 10036
[2]Dominick P. Purpura Department of Neuroscience, Albert Einstein College of Medicine, Bronx, NY 10461

The anti-malarial drug quinine and its quaternary derivative *N*-benzylquininium (BQ^+) have been shown to inhibit gap junction (GJ) channels with specificity for Cx50 over its closely related homologue Cx46. Here, we examined the mechanism of BQ^+ action using undocked Cx46 and Cx50 hemichannels, which are more amenable to analyses at the single-channel level. We found that BQ^+ (300 µM–1 mM) robustly inhibited Cx50, but not Cx46, hemichannel currents, indicating that the Cx selectivity of BQ^+ is preserved in both hemichannel and GJ channel configurations. BQ^+ reduced Cx50 hemichannel open probability (P_o) without appreciably altering unitary conductance of the fully open state and was effective when added from either extracellular or cytoplasmic sides. The reductions in P_o were dependent on BQ^+ concentration with a Hill coefficient of 1.8, suggesting binding of at least two BQ^+ molecules. Inhibition by BQ^+ was voltage dependent, promoted by hyperpolarization from the extracellular side and conversely by depolarization from the cytoplasmic side. These results are consistent with binding of BQ^+ in the pore. Substitution of the N-terminal (NT) domain of Cx46 into Cx50 significantly impaired inhibition by BQ^+. The NT domain contributes to the formation of the wide cytoplasmic vestibule of the pore and, thus, may contribute to the binding of BQ^+. Single-channel analyses showed that BQ^+ induced transitions that did not resemble pore block, but rather transitions indistinguishable from the intrinsic gating events ascribed to loop gating, one of two mechanisms that gate Cx channels. Moreover, BQ^+ decreased mean open time and increased mean closed time, indicating that inhibition consists of an increase in hemichannel closing rate as well as a stabilization of the closed state. Collectively, these data suggest a mechanism of action for BQ^+ that involves modulation loop gating rather than channel block as a result of binding in the NT domain.

INTRODUCTION

Connexins are a multi-gene family of proteins that form gap junction (GJ) channels. These cell–cell channels mediate direct signaling between cells and are formed by the docking of two hemichannels, one from each of two contacting cells. Each hemichannel is a hexamer of connexin subunits (Willecke et al., 2002), with a topology that consists of four transmembrane (TM) domains (TM1–TM4) and two extracellular loops (E1 and E2) with the amino and carboxy termini located intracellularly. In addition to functioning as GJ channels, connexins can function as hemichannels in the absence of docking. Genetic and molecular studies indicate that both hemichannels and GJ channels formed by different connexins play important roles in many aspects of tissue homeostasis, a view highlighted by the association of a growing list of human diseases with mutations in connexin genes (Zoidl and Dermietzel, 2010; Pfenniger et al., 2011).

Connexin channels exhibit diverse gating and permeability characteristics, suggesting that the biophysical properties of connexins are important in conferring tissue-specific function. Several studies have shown that alteration in biophysical properties as a result of mutations in connexin genes likely contributes to human diseases (DeRosa et al., 2007; Gerido et al., 2007; Mese et al., 2008; Minogue et al., 2009; Sánchez et al., 2010). However, the molecular mechanisms underlying essential connexin channel functions, such as gating and permeation, are poorly understood. Pharmacological agents have been invaluable tools for structure–function studies of ion channels, in general, having aided in the identification of voltage sensors and pore structures. Many small molecules and peptides are known to inhibit connexin channels, but examination of their mechanisms of action has been hampered in GJ channels because of their inaccessibility to direct patch recording in cell-attached and excised-patch configurations, thereby making it difficult to obtain stable single-channel recordings and precluding examination of inhibitor effects in a cell-free environment.

In this study, we used undocked Cx46 and Cx50 hemichannels expressed in *Xenopus laevis* oocytes to examine

Correspondence to Miduturu Srinivas: msrinivas@sunyopt.edu

Abbreviations used in this paper: BQ^+, *N*-benzylquininium; GJ, gap junction; NT, N terminal/terminus; P_o, open probability; TM, transmembrane; wt, wild type.

The Rockefeller University Press $30.00
J. Gen. Physiol. Vol. 139 No. 1 69–82
www.jgp.org/cgi/doi/10.1085/jgp.201110678

the mechanism of action of *N*-benzylquininium (BQ^+), a charged quaternary derivative of the anti-malarial drug quinine. Previous studies showed that quinine and mefloquine inhibit GJ channels in a connexin-specific manner (Srinivas et al., 2001; Cruikshank et al., 2004). Inhibition was found to be strong for GJs formed by Cx50 and Cx36, but not other connexins (e.g., Cx43 and Cx46, a close homologue of Cx50) at comparable concentrations. Inhibition of Cx50 GJs by quinine was dependent on extracellular and intracellular pH, consistent with a binding site that was accessed from the cytoplasm (Srinivas et al., 2001). In support, BQ^+ inhibited Cx50 GJs only when applied intracellularly via patch pipettes. However, whether the binding site for these drugs was in the pore or elsewhere in the channel could not be assessed. Here, using Cx50 hemichannels, we found a robust, concentration-dependent inhibition of macroscopic and single-hemichannel currents by BQ^+. Application of BQ^+ to Cx46 showed poor inhibition in hemichannels and GJ channels, indicating that BQ^+ maintains the same specificity for Cx50 over Cx46 in both docked and undocked channel configurations. Also, we could apply BQ^+ to the cytoplasmic and extracellular faces of single Cx50 hemichannels in excised patches and determine the sidedness of action and effects on unitary conductance and open/closed dwell times. Our results indicate that the effect of BQ^+ is voltage dependent in a manner consistent with movement in the electric field and binding within the channel pore. The effect, however, did not appear to be open hemichannel block, but rather modulation of gating. Studies with chimeric hemichannels in which specific domains of Cx50 were exchanged with corresponding domains of Cx46 indicated that the N terminus (NT), which has been identified by biophysical and structural studies to constitute the cytoplasmic aspect of the pore of connexin channels (Verselis et al., 1994; Oh et al., 1999; Purnick et al., 2000; Dong et al., 2006; Maeda et al., 2009), plays an important role in conferring inhibition by BQ^+.

MATERIALS AND METHODS

Drugs

BQ^+ was obtained from Sigma-Aldrich. 20-mM stock solutions were prepared in distilled water just before use. Drugs were applied at the indicated concentrations using a gravity-fed perfusion system or applied via patch pipettes after dissolving in the internal solution.

Construction of chimeric constructs and site-directed mutagenesis

The coding sequence of mouse Cx50 was cloned into the HindIII and BamHI sites of a PSP64T transcription vector (provided by T. White, SUNY, Stony Brook, NY). Rat Cx46 was cloned into the EcoR1 and HindIII sites of pGEM vector. To construct chimeric channels, a silent BamHI site was engineered in the Cx50 and Cx46 coding sequences at the beginning of TM1 using oligonucleotide primers and the PCR using the QuickChange mutagenesis kit (Agilent Technologies) according to the manufacturer's protocol. Restriction digests of the new constructs and ligation reactions were made as described previously (Trexler et al., 1999). We constructed two chimeric hemichannels, designated as Cx46*Cx50NT, which has the sequence of the N-terminal (NT) region (Met 1-Arg23) of Cx46 replaced with that of Cx50, and the reverse chimera Cx50*Cx46NT, in which the Cx50NT sequence was replaced with that of Cx46. All structures were sequenced entirely.

Expression of connexins in *Xenopus* oocytes

Expression of connexins in *Xenopus* oocytes, synthesis of RNA, and preparation and injection of oocytes have been described previously (Trexler et al., 1996, 1999). In brief, mRNA was prepared from appropriately linearized plasmid DNA with the mMessage mMachine SP6 RNA kits (Invitrogen) according to the manufacturer's protocol and purified using QIAquick PCR purification columns (QIAGEN). Each oocyte was injected with 50–100 nl mRNA. Injected oocytes were maintained at 16–18°C in a modified ND96 solution containing (in mM): 100 NaCl, 2 KCl, 1 $MgCl_2$, 1.8 $CaCl_2$, 10 glucose, 10 HEPES, and 5 pyruvate, pH adjusted to 7.6.

Electrophysiological recordings

For recordings of macroscopic hemichannel currents, *Xenopus* oocytes were placed in a polycarbonate RC-1Z recording chamber (Warner Instruments) consisting of a slot-shaped chamber connected at opposite ends with inflow and outflow compartments. A suction tube was placed in the outflow compartment as well as agar bridges containing ground wires. Perfusion solutions consisted of (in mM): 100 NaCl, 1 $MgCl_2$, and 10 HEPES, to which Ca^{2+} concentration was adjusted to desired levels. Recordings were obtained with a GeneClamp 500 two-electrode voltage clamp (Axon Instruments). Both current-passing and voltage-recording pipettes contained 1 M KCl. For recordings of macroscopic junctional currents, N2A cells were transfected with cDNA corresponding to individual connexins. Junctional currents were measured using the dual whole cell patch-clamp technique as described previously (Srinivas et al., 2001).

For patch-clamp recordings of single-hemichannel currents, *Xenopus* oocytes were manually devitellinized in a hypertonic solution consisting of (in mM) 220 Na aspartate, 10 KCl, 2 $MgCl_2$, and 10 HEPES, and then placed in the ND96 solution for recovery. Oocytes were then individually moved to a recording chamber (RC-28; Warner Instruments) containing the patch pipette solution (IPS), which consisted of (in mM): 140 KCl, 1 $MgCl_2$, 5 HEPES, 1 $CaCl_2$, and 3 EGTA, pH adjusted to 8.0 with KOH. The bath compartment was connected via a 3-M agar bridge to a ground compartment containing the same IPS solution. After excision of patches containing single hemichannels, instrumentation offsets were manually corrected in the absence of an applied voltage. In all electrophysiological recordings, data were acquired with AT-MIO-16X D/A boards from National Instruments using custom acquisition software (written by E.B. Trexler, Mt. Sinai School of Medicine, New York, NY). In patch-clamp experiments, currents were typically filtered at 1 kHz and data were acquired at 5 kHz.

Data analysis

Single-hemichannel records from voltage steps and ramps were leak subtracted by measuring the leak current during full-closing events and extrapolating linearly with voltage. Single-channel recordings were analyzed with Clampfit (Molecular Devices). To determine single-channel amplitude, all-point amplitude histograms were constructed and fit to Gaussian functions. To determine channel open probability (P_o) and open and closed dwell times, current traces were idealized using the half-amplitude threshold-crossing method in Clampfit. Dwell-time histograms were plotted

on a logarithmic abscissa and were fit using the maximum likelihood method. Cx50 channels gate strongly to subconductance states at large hyperpolarized voltages, such that P_o decreased from ~0.95 at −70 mV to <0.3 at a voltage of −120 mV. For single-channel analyses of the effects of BQ^+, we obtained dwell-time histograms at a potential of −70 mV in the presence of EGTA to chelate Ca^{2+}, conditions under which residence in subconductance states or fully closed states was infrequent and brief. Application of BQ^+ induced only transitions to the fully closed state, and any brief subconductance transitions were excluded from analysis. The single-channel current in the closed state induced by BQ^+ showed continuous fluctuations from the baseline that varied considerably in duration and in amplitude, and often did not cross the half-amplitude threshold. Dwell-time distributions, therefore, were constructed by ignoring the majority of these fluctuations. Also, events briefer than 5 msec were excluded from analysis.

For quantitative analysis of inhibition, the fraction of inhibition produced by BQ^+ (F_{BQ}) was measured, defined as $F_{BQ} = 1 - P_{o,BQ}/P_{o,control}$, where $P_{o,BQ}$ and $P_{o,control}$ represent the single-channel P_o in BQ^+ and in control, respectively. The IC_{50} values and Hill slopes were estimated by fitting the relationship between F_{BQ} and BQ^+ concentration to the Hill equation at a given voltage.

$$F_{BQ} = \frac{[BQ]^n}{[BQ]^n + IC_{50}{}^n},$$

where IC_{50} is the concentration of BQ^+ that causes a fractional inhibition of 50%, n is the Hill coefficient, and [BQ] is the inhibitor concentration.

RESULTS

Effect of BQ^+ on macroscopic Cx50 hemichannel currents

Fig. 1 A shows the effect of BQ^+ on Cx50 hemichannel currents in an oocyte voltage clamped to a holding potential of −70 mV. Lowering extracellular Ca^{2+} from 1.8 mM to 200 µM and substituting NaCl with KCl led to the development of a large inward current in Cx50-expressing oocytes, as shown previously (Srinivas et al., 2006). Bath application of BQ^+ produced a rapid reduction in the inward current in a concentration-dependent manner. In the illustrated examples, BQ^+ at concentrations of 500 µM and 1 mM decreased the current at a holding potential of −70 mV by 48 and 78%, respectively (see Fig. 1 B). Inhibition was readily reversed upon washout. To test if the inhibitory action of BQ^+ on hemichannel currents shows connexin specificity, we examined the effects of BQ^+ on Cx46 hemichannels. Quinine, the "parent compound," was shown to inhibit Cx50, but not Cx46, GJ channels at concentrations of 30 µM to 1 mM (Srinivas et al., 2001). Bath application of BQ^+ had little or no effect on Cx46 hemichannel currents at 500 µM and a modest decrease at 1 mM. Comparison of mean changes observed in Cx46- and Cx50-expressing oocytes is summarized in Fig. 1 B. We also tested the effect of BQ^+ on Cx46 and Cx50 GJ channels and found that the drug was similarly selective for Cx50 (Fig. 1 C). These results indicate that the action of BQ^+ is connexin specific and that specificity is not affected by hemichannel docking. Thus, the binding site for BQ^+ is likely preserved in both docked and undocked channel configurations.

In addition to reversible inhibition, we found that BQ^+ produced an additional effect on membrane currents in Cx50-expressing oocytes. As evident from the recording shown in Fig. 1 A, the rapid inhibition of Cx50 hemichannel currents by 500 µM BQ^+ was followed by a modest increase in current in the continued

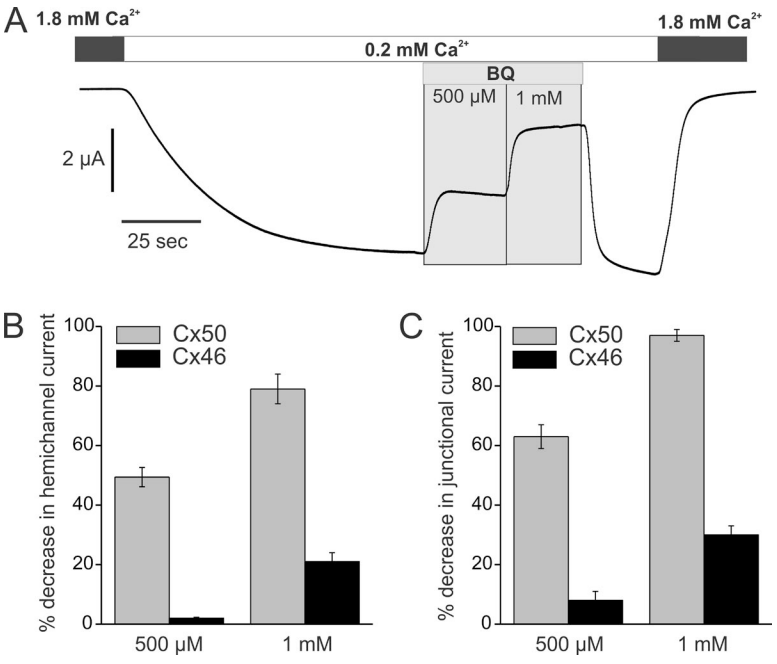

Figure 1. Connexin-selective inhibition of hemichannel currents by BQ^+. (A) Membrane currents in a Cx50-expressing oocyte voltage clamped at −70 mV. Reduction of Ca^{2+} from 1.8 to 0.2 mM in a KCl solution promoted robust opening of Cx50 hemichannels, evident by the development of a large inward current. The application of 500 µM and 1 mM BQ^+ in the continued presence of 0.2 mM Ca^{2+} caused a rapid and concentration-dependent reduction in current at −70 mV, an effect that was reversible upon washout. (B and C) Cx46 hemichannels were only moderately affected by 500 µM and 1 mM BQ^+. Bar graph shows a comparison of the decrease in Cx46 (black bars) and Cx50 (gray bars) hemichannel currents caused by 500 µM and 1 mM BQ^+. Because Cx46 activates only at positive voltages, tail current amplitudes were measured at −70 mV after 5-s depolarizing voltage steps to +50 mV. Each bar represents the mean ± SEM of six oocytes. (C) Selective inhibition by BQ^+ of GJ channels formed by Cx50 but not Cx46. Bars represent the mean ± SEM of the decrease in junctional currents caused by the addition of BQ^+ to patch pipettes (*n* ranged from 4 to 15). The decrease caused by BQ^+ was measured after 12 min of achieving whole cell configuration.

presence of the drug. The slow increase was not evident in 1mM BQ^+. However, the current after washout was larger compared with levels before BQ^+ application (Fig. 1 A). The magnitude of BQ^+-induced potentiation was variable among Cx50-expressing oocytes, ranging from a 1.2–1.5-fold increase, but was observed in all Cx50-expressing oocytes ($n = 27$). This secondary increase in current after inhibition at lower BQ^+ concentrations was not observed in single Cx50 hemichannel recordings from excised patches. These data indicate that the increased current observed macroscopically likely resulted from recruitment of hemichannels to the oocyte membrane. We did not pursue additional studies to determine the mechanism of hemichannel recruitment by BQ^+.

Effect of BQ^+ on single Cx50 hemichannels

To determine the concentration and voltage dependence of BQ^+ action, we recorded from single Cx50 hemichannels in excised patches and exposed them to a range of BQ^+ concentrations at various potentials. Use of single-hemichannel recordings in excised patches avoided the secondary effects related to hemichannel recruitment. Fig. 2 (top) shows an example of a Cx50 hemichannel recording obtained from an excised outside-out patch held at a membrane potential of −50 mV with and without the addition of 500 µM BQ^+ to the bath. Extracellular Ca^{2+} was maintained at submicromolar levels by the addition of EGTA. Before application of BQ^+, the Cx50 hemichannel remained predominantly open (P_o of ∼0.98). Bath application of BQ^+ induced frequent transitions to a fully closed state. Inhibition of hemichannel activity was observed rapidly upon the addition of BQ^+ to the bath and was readily reversed upon switching back to a drug-free solution. In the example shown, the P_o of the Cx50 hemichannel was reduced from 0.98 to 0.40 and recovered to 0.92 after washout (see all-points histograms; Fig. 2, bottom). Interestingly, BQ^+ did not alter the amplitude of the fully open single-hemichannel current. All-points amplitude histograms constructed from current traces in the presence of BQ^+ and after washout show peaks corresponding to the fully open state at −27.5 and −28 pA, respectively. However, subconductance states are evident in the spread of the amplitude histograms in Figs. 2 and 3 in the presence of BQ^+, which likely arise from the frequent fluctuations induced by BQ^+, as described below.

Concentration dependence of BQ^+ action

To examine the effects of BQ^+ on dwell times in open and closed states, we recorded from single hemichannels in outside-out patches for longer durations (60 s) in the presence of BQ^+ at various concentrations. Fig. 3 shows 15-s segments of current traces recorded from patches held at −70 mV in the absence of BQ^+ and in the presence of 300 µM, 500 µM, and 1 mM BQ^+ applied to the extracellular face of the hemichannel. As evident from the recordings and amplitude histograms shown to the right of each trace, residence in the fully open state became less frequent with higher BQ^+ concentrations. For the recording shown in Fig. 3, P_o was reduced from 0.95 in the absence of BQ^+ to 0.58 at 300 µM, 0.37 at 500 µM, and 0.12 at 1 mM of BQ^+ (see Fig. 6 for means and SEM).

Single-hemichannel recordings also revealed that the BQ^+-induced transitions between open and fully closed states are complex, like the intrinsic gating transitions characteristic of loop gating (selected segments, depicted by boxed regions in Fig. 3, are shown below each trace on an expanded time scale). Loop gating, originally described

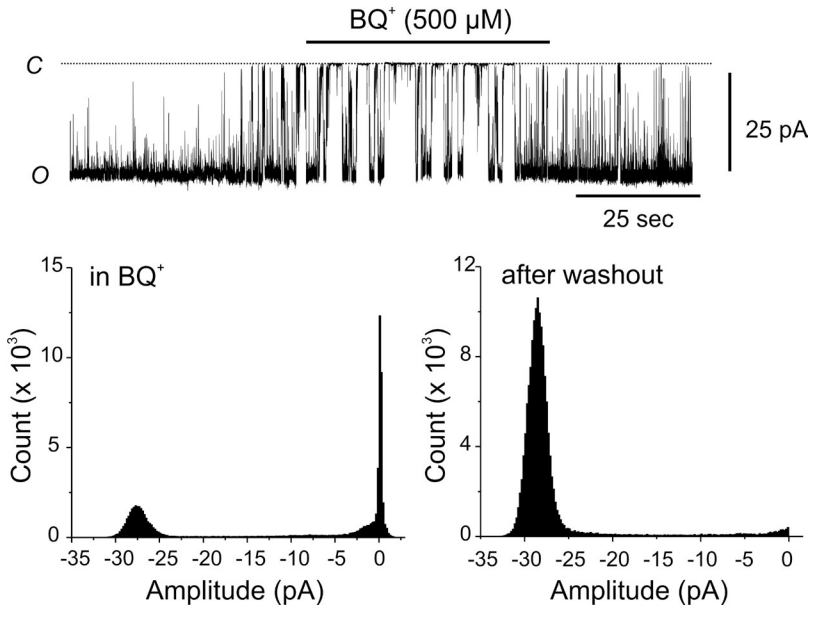

Figure 2. BQ^+ reduces the P_o of Cx50 hemichannels in excised patches. Shown on top is a recording of a single Cx50 hemichannel in an outside-out configuration at a membrane potential of −50 mV. The application of 500 µM BQ^+ to the extracellular face of the hemichannel caused a robust reduction in the P_o of the hemichannel, evident by transitions of the hemichannel to the fully closed state (dotted line). The reduction in P_o was reversible upon washout of BQ^+. Amplitude histograms shown in the bottom panels indicate that the amplitude of the fully open state was not affected in the presence of 500 µM BQ^+. Histograms were obtained from the current recording during the application of BQ^+ (left) and after washout of BQ^+ (right).

in Cx46 hemichannels (Trexler et al., 1996), is a property common to all connexin hemichannels and GJ channels, and is characterized by transitions that pass through a series of transient subconductance states en route to full opening/closure (Trexler et al., 1996, 1999). In submicromolar Ca^{2+} at −70 mV in the absence of BQ^+, single Cx50 hemichannels exhibit loop-gating transitions (see boxed region in Fig. 3 for the control trace), but the frequency with which they occur is low and dwell times in the fully closed state are brief. The addition of BQ^+ led to a dramatic increase in the frequency of closures indistinguishable from loop gating. Moreover, the closed-state current exhibited frequent noisy fluctuations, which is also a characteristic of loop gating. These fluctuations were observed at all BQ^+ concentrations and were most evident at concentrations that caused reductions in P_o that were near half-maximal (in Fig. 3, see spread in the histograms in away from the fully closed state at 500 μM BQ^+).

We sought to analyze the effect of increasing BQ^+ concentrations on the mean open and closed dwell times of Cx50 hemichannels to determine additional details of the mechanism of inhibition. Whereas open times were rather discernable, closed times were more difficult to assess because of the continuous current fluctuations. These fluctuations varied in complexity, duration, and amplitude, but often did not reach half-height amplitude or were too brief (<5 msec), criteria we set for considering an opening event (see Materials and methods). Fig. 4 shows results obtained by pooling measurements from several different outside-out patches at each concentration of BQ^+ applied to the extracellular face of the hemichannel. We chose a membrane potential of −70 mV, at which loop gating was infrequent in the

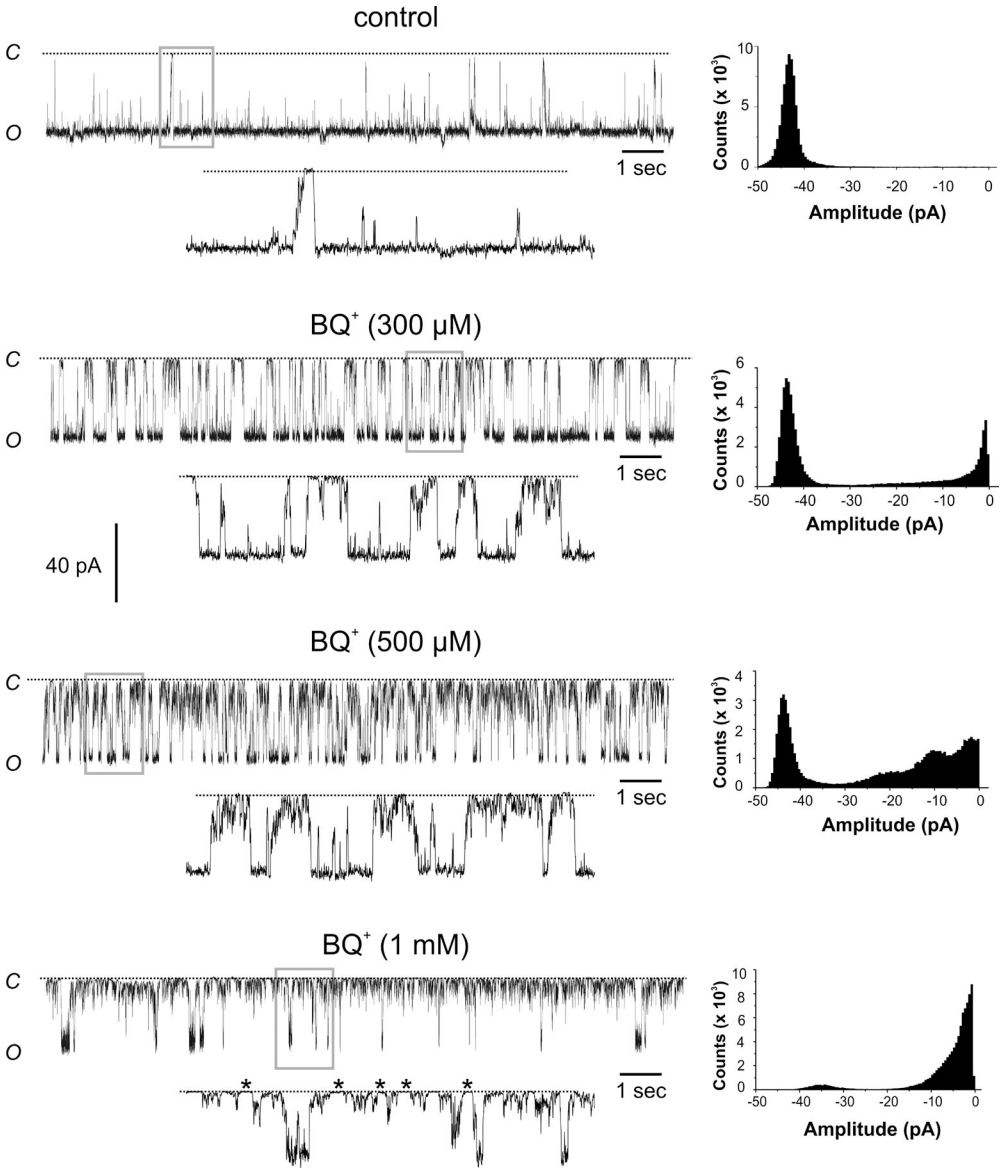

Figure 3. The decrease in P_o of Cx50 hemichannels caused by BQ^+ is concentration dependent and is a result of an increase in loop gating. Recordings of single Cx50 hemichannels before and after the addition of 300 μM, 500 μM, and 1 mM BQ^+ applied to the extracellular face. 15-s segments of current traces recorded at a membrane potential of −70 mV along with corresponding all-points histograms obtained from longer (30-s) recordings (right of each trace) are shown. In the absence of BQ^+, Cx50 hemichannels are predominantly open (*O*) at −70 mV, with occasional brief transitions to the fully closed state (*C*). The application of BQ^+ caused a reduction in the P_o, evident as an increase in the frequency of transitions to the fully closed state. Views of the current traces recorded with or without BQ^+ at an expanded time scale. The boxed regions indicate the segments of the traces that were expanded. In the presence of BQ^+, the transitions between open and closed states exhibit slow kinetics, indistinguishable from intrinsic gating events (see control trace) attributed to loop gating. Asterisks show more stable closing events in 1 mM BQ^+.

absence of BQ^+. Histograms of open times without or with 500 μM BQ^+ were fit well by single exponentials with time constants of 738 and 71 msec, respectively (Fig. 4 A). Mean open times over a range of BQ^+ concentrations are shown in Fig. 4 B. BQ^+ decreased the mean open time in a concentration-dependent manner, consistent with BQ^+ binding to the open state of the Cx50 hemichannel and promoting closure. Closed-state durations, as defined by the criteria outline above, were also affected by BQ^+. In the absence of BQ^+, closed durations were typically brief and described by a single exponential, giving a mean closed time of 22 msec. In the presence of 500 μM BQ^+, the mean closed-time distribution, which included many fluctuations, was considerably broadened but could be fit by a single exponential that yielded a mean closed time that increased to 141 msec. The increase in mean closed times was concentration dependent (Fig. 4 B), suggesting that the binding of BQ^+ leads to stabilization of the closed state. However, these results should be interpreted with caution, considering the problematic nature of quantifying the closed durations.

Voltage-dependent inhibition of Cx50 channels by BQ^+

To determine the voltage dependence of BQ^+ action, we recorded from excised outside-out patches containing single Cx50 hemichannels held at different holding potentials with and without the addition of 500 μM BQ^+ to the extracellular side of the membrane (Fig. 5). As expected of a binding site that is within the membrane's electric field, the inhibition produced by BQ^+ increased progressively with hyperpolarization, which would tend to drive BQ^+ into the hemichannel. In the recording shown, P_o decreased from 0.98 to 0.72 at −50 mV, from 0.96 to 0.38 at −70 mV, and from 0.87 to 0.22 at −90 mV (Fig. 5). In contrast, at voltages positive to −30 mV, BQ^+ produced little change in P_o compared with control (compare traces at −30 and +20 mV, control vs. BQ^+).

The P_o values at voltages between +20 and −110 mV were used to calculate fractional inhibition (F_{BQ}), defined as $1\text{-}Po_{BQ}/Po_{control}$. Fig. 6 A shows a plot of F_{bq} versus membrane potential at BQ^+ concentrations of 300 μM, 500 μM, and 1 mM. A progressive rightward shift in the F_{bq}–V curve can be seen with increasing BQ^+ concentration, reflecting both the concentration and voltage dependence

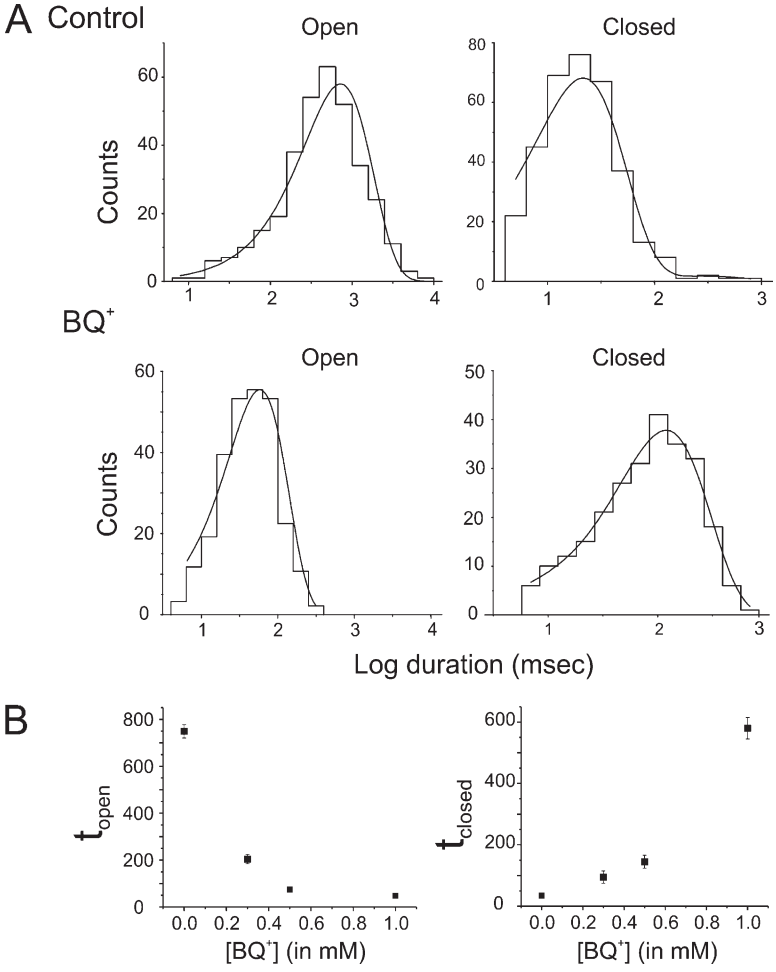

Figure 4. BQ^+ alters both open- and closed-time distributions of Cx50 hemichannels. (A) Representative open- and closed-time distributions at −70 mV in the absence (control) and the presence of 500 μM BQ^+ plotted on a logarithmic abscissa. Lines are single-exponential fits to the histograms. (B) Concentration dependence of mean open (left) and mean closed (right) times.

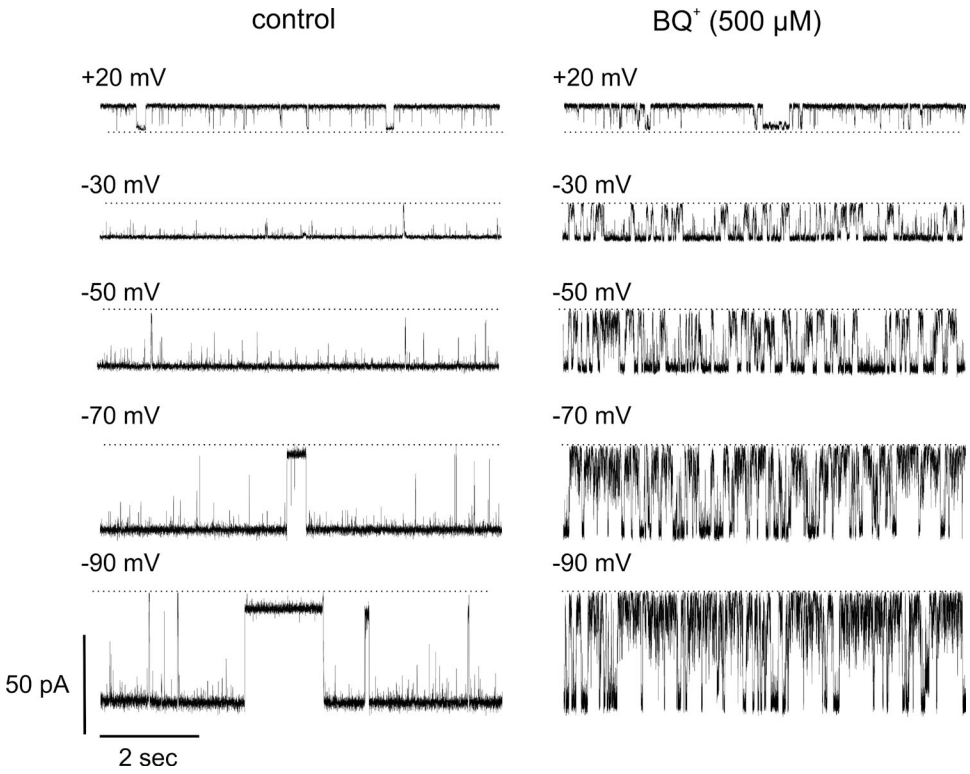

Figure 5. Voltage-dependent inhibition of Cx50 hemichannels by extracellular BQ^+ suggests a binding site in the pore. Recordings of single-hemichannel currents in excised patches in control (left) and in 500 μM BQ^+ (right) at membrane potentials of +20, −30, −50, −70, and −90 mV are shown. BQ^+ was applied to the extracellular side of the hemichannel. Dashed lines in the current traces indicate the closed state. In the absence of BQ^+, Cx50 hemichannels predominantly reside in the open state at voltages between +20 and −70 mV. With further hyperpolarization, Cx50 hemichannels tend to gate to long-lived subconductance states (see trace at −90 mV). The application of 500 μM BQ^+ to the extracellular side caused strong inhibition at large hyperpolarizing voltages, but little inhibition at smaller hyperpolarizing voltages (compare P_o in BQ^+ at −30 and −90 mV). An increase in inhibition with hyperpolarization, which tends to drive BQ^+ into the hemichannel, is suggestive of a binding site within the aqueous pore.

of inhibition. The solid lines are fits of the data points in the three curves to a Boltzmann equation assuming little or no permeation of BQ^+ at voltages above −90 mV. The $V_{1/2}$ values decreased with BQ^+ concentration from 86 mV at 300 μM to −53 mV at 500 μM and −30 mV at 1 mM. The slope of the F_{BQ}–V relationship ranged from −24 to −26 mV^{-1}. The relationship between inhibition, BQ^+ concentration, and the membrane potential can also be seen in Fig. 6 B, where the F_{BQ} values are replotted as a function of concentration at voltages of −30, −50,

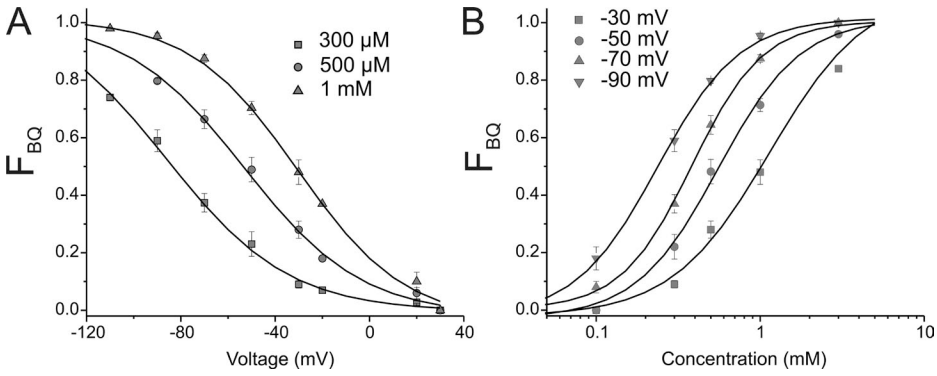

Figure 6. Concentration and voltage dependence of the inhibition of single Cx50 hemichannels by BQ^+ applied to the extracellular side. (A) Plots of fractional inhibition (F_{BQ}) versus V_m at BQ^+ concentrations of 300 μM, 500 μM, and 1 mM demonstrate the voltage dependence of inhibition. Solid lines are fits to a Boltzmann equation. The mean $V_{1/2}$ values from Boltzmann analysis are −86, −53, and −30 mV, with slope factors of 26, 25, and 23 mV^{-1} for 300 μM, 500 μM, and 1 mM BQ^+, respectively. (B) Plots of fractional inhibition (F_{BQ}) versus BQ^+ concentrations of −30, −50, −70, and −90 mV. The solid lines are fits to the Hill equation, with K_d values of 1.14, 0.556, 0.38, and 0.24 mM and Hill slopes of 1.6, 1.7, 1.9, and 1.7 at −30, −50, −70, and −90 mV, respectively.

−70, and −90 mV. BQ^+ inhibits Cx50 hemichannels in a narrow concentration range at all voltages. At a low concentration of 100 μM, BQ^+ produced significant inhibition only at large hyperpolarizing voltages, whereas at a concentration of 1 mM, BQ^+ reduced hemichannel openings even at small hyperpolarizing voltages. The solid curves in Fig. 6 B are fits of the data according to the Hill equation (see Materials and methods). The best-fit parameters were as follows: IC_{50} = 1, 0.72, 0.34, and 0.2 mM, and nH = 1.8, 1.6, 1.9, and 1.7 at −30, −50, −70, and −90 mV, respectively. The dissociation constants decrease at higher holding potentials, confirming the voltage-dependent inhibition of single-hemichannel currents shown in Fig. 5. The Hill coefficients at all voltages are close to 2, suggesting that binding of at least two BQ^+ molecules may be required for inhibition.

The electrical distance traversed by an impermeant blocker within the membrane electric field can be estimated using the Woodhull model (Woodhull, 1973). Validation that a blocker is permeant may be obtained by studying the relief of inhibition at large voltages: for a permeant, positively charged molecule applied to the extracellular side, hyperpolarization is expected to enhance inhibition, but the application of stronger hyperpolarizing voltages may lead to relief of inhibition as the molecule is driven out of the pore. However, assessment of the relief of inhibition was made difficult by strong gating of Cx50 hemichannels to subconductance states at large negative voltages exceeding −110 mV. Patches were also unstable at large inside negative voltages preventing long-duration recordings that are required for the assessment of fractional inhibition. Thus, we cannot explicitly state that BQ^+ permeates based on relief of inhibition, but the large size of the pore together with accessibility to binding from either side (see below) support permeation of BQ. Although the Woodhull model is unlikely to be valid here, the estimation of electrical distance using this model may be useful for comparison among different connexins or inhibitors acting by a similar mechanism. A plot of log (IC_{50}) versus membrane potential appeared to have a linear relationship

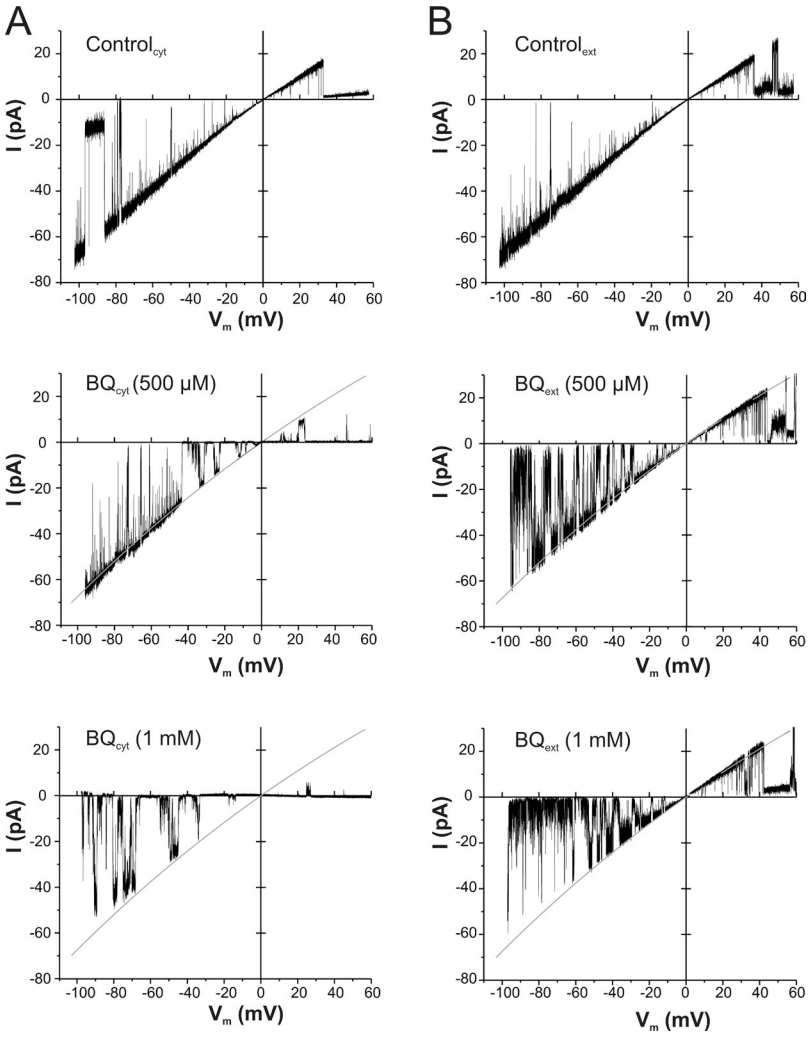

Figure 7. Voltage dependence of inhibition by BQ^+ applied to the cytoplasmic side of Cx50 hemichannels. Single-channel I-V relationships in control (top), in 500 μM BQ^+ (middle), and in 1 mM BQ^+ (bottom) applied either to the cytoplasmic side (A) or extracellular side (B) of Cx50 hemichannels. I-V relations in A and B were obtained in response to 8-s voltage ramps from −100 to +50 mV applied to excised inside-out patches and outside patches, respectively. Inhibition produced by cytoplasmic application of BQ^+ (BQ^+_{cyt}) is promoted by depolarization, a voltage dependence that is opposite to that observed when BQ^+ is applied to the extracellular side, indicating a binding site located in the pore. In addition, inhibition by intracellular BQ^+, especially at a 1-mM concentration, occurs even at strong inside-negative voltages. Hyperpolarizing voltages are expected to prevent entry of BQ^+ on the intracellular side into the pore, suggesting that the binding site is closer to the cytoplasmic end of the hemichannel. Solid lines superimposed on the current traces in BQ^+ represent exponential fits to the open-state current in the absence of BQ^+ to illustrate the decrease in conductance at high, but not lower, BQ^+ concentrations (see Results).

(not depicted). Fits of the data to the Woodhull equation, assuming no permeation at voltages less than −90 mV, indicated that extracellularly applied BQ^+ sensed a substantial fraction of the field ($\delta = 0.72$), suggesting that the binding site for BQ^+ is closer to the cytoplasmic end of the hemichannel.

Inhibition by BQ^+ from the cytoplasmic side

The voltage dependence of inhibition suggests that the BQ^+-binding site may be in the pore toward the cytoplasmic end. However, voltage dependence of inhibition may also arise from interactions of permeant ions with BQ^+ or from state-dependent binding of the BQ^+. To further test that the binding site for BQ^+ is in the hemichannel pore, we examined the voltage dependence of inhibition when BQ^+ was applied to the cytoplasmic side using excised inside-out patches. The expectation was that for binding in the pore, the polarity of voltage-dependent inhibition would now occur at increasingly positive, rather than negative, membrane voltages. Fig. 7 compares the voltage dependence of inhibition using voltage ramps applied to single Cx50 hemichannels with BQ^+ applied either to extracellular (i.e., to outside-out patches) or the cytoplasmic side (inside-out patches). The I-V relations shown were obtained by applying voltage ramps from −100 to + 50 mV to excised patches that were exposed to BQ^+ concentrations of 500 μM (Fig. 7, middle traces) or 1 mM (bottom traces). With BQ^+ on the extracellular side, closure was promoted by membrane hyperpolarization (Fig. 7 B). In contrast, upon the application of BQ^+ to the cytoplasmic side, hemichannels now closed strongly with membrane depolarization; openings were typically observed at hyperpolarizing voltages (Fig. 7 A). At a lower concentration of BQ^+ (500 μM; Fig. 7 A, middle trace), hemichannel closure was promoted by depolarization to voltages beyond −40 mV. A similar trend was observed with 1 mM BQ^+ on the cytoplasmic side, with the only major difference being a shift in the voltage dependence of inhibition to more negative voltages.

Fig. 7 also shows that BQ^+ produces a modest reduction in unitary conductance of the fully open state at high concentrations. In the absence of BQ^+, single Cx50 hemichannels are predominantly open and exhibit an ∼2:1 inward rectification of the open hemichannel current and a slope conductance of ∼450 pS measured at 0 mV.

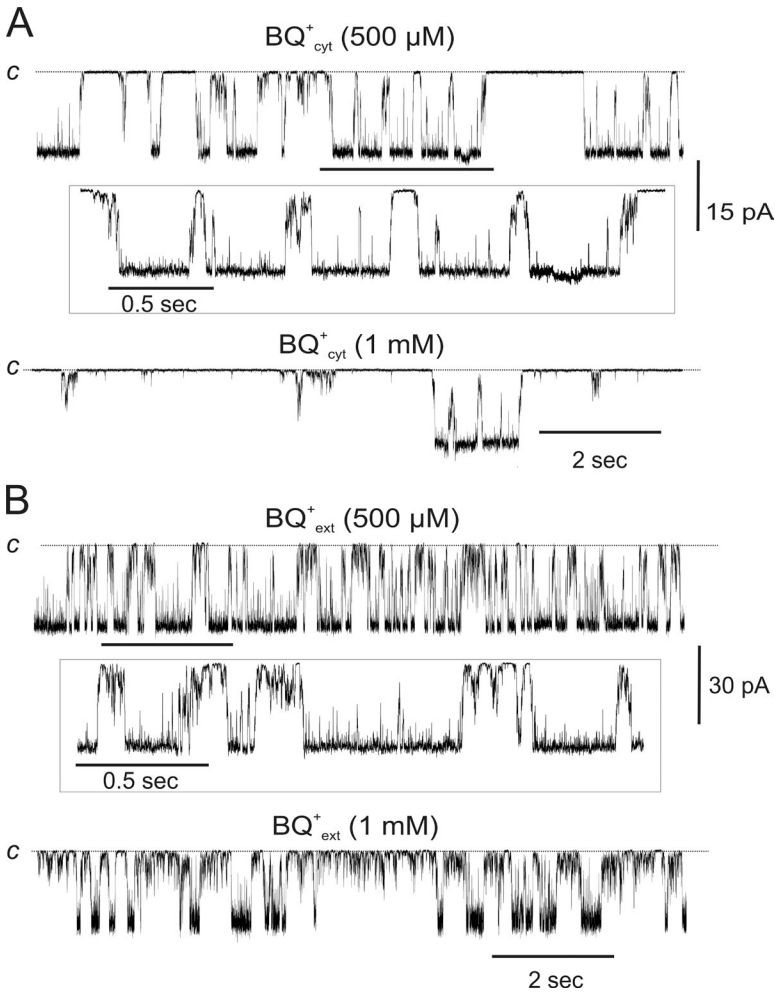

Figure 8. Differences in BQ^+ action when applied to the cytoplasmic and the extracellular sides. Recordings of a single Cx50 hemichannel with BQ^+ added to the cytoplasmic side (A) and the extracellular side (B) obtained from separate patches are shown. Membrane potential was held constant at −30 mV in A and −50 mV in B. Regardless of the side of application, BQ^+ increased loop-gating transitions. All transitions between the open and closed state are slow in kinetics, typical of loop gating, as shown in the expanded views of the current traces recorded at 500 μM BQ^+ applied to the cytoplasmic and extracellular side (see boxed regions). The solid black line indicates the segments of the traces that were expanded. Notably, the noisy fluctuations from the closed state (dotted line) that characterized BQ^+ action when applied to the extracellular side were much less prominent when BQ^+ was applied to the cytoplasmic side. Currents were filtered at 1 kHz, and data were acquired at 5 kHz.

The slope conductance of the fully open state in 500 μM BQ^+ was similar to control (445 ± 15 pS; $n = 5$). In contrast, the slope conductance at 1 mM BQ^+ was significantly lower than control values (338 ± 26 pS). This reduction occurred regardless of whether the BQ^+ was applied to the cytoplasmic or the extracellular face of the hemichannel. Similar results were found in six other patches, with current amplitudes in the presence of 1 mM BQ^+ reduced by 26.2 ± 4% relative to control.

The application of BQ^+ to the cytoplasmic side, similar to the application to the extracellular side, induced full closing transitions resembling loop gating. The marked increase in the incidence of loop-gating transitions is shown in the recordings from inside-out patches illustrating the effect of cytoplasmic BQ^+ at a membrane potential of −50 mV (Fig. 8 A). However, the closed state appeared to be more stable in that the noisy fluctuations were less prominent than when BQ^+ was applied to the extracellular side. This difference in BQ^+ action is illustrated in Fig. 8, which shows a comparison of single-channel recordings obtained in 500 μM and 1 mM BQ^+ applied either to the cytoplasmic (Fig. 8 A) or the extracellular (Fig. 8 B) side.

The NT is important for the effect of BQ^+

Because our data suggests that BQ^+ binds in the pore toward the cytoplasmic end of the hemichannel, we examined whether the amino terminus (NT), which is believed to constitute the cytoplasmic vestibule of the pore, is important for the inhibition produced by BQ^+. Because Cx46 hemichannels were less sensitive to BQ^+, we constructed chimeric hemichannels composed of Cx46 with the NT domain replaced with that of Cx50, Cx46*50NT, and the reciprocal chimera, Cx50*46NT, composed of Cx50 with the NT domain replaced with that of Cx46. Both chimeric hemichannels produced membrane currents when the cRNAs were injected into *Xenopus* oocytes. Currents in oocytes expressing Cx46*50NT and Cx50*46NT showed a reversible decrease upon the application of BQ^+ to the bath (not depicted). Concentration–response curves for the inhibition of Cx46*50NT and Cx50*46NT channels compared with Cx50 and Cx46 wild-type (wt) channels are shown in Fig. 9. Currents in oocytes expressing Cx46*50NT were significantly affected by BQ^+ (300 μM to 1 mM). The IC_{50} value for inhibition of Cx46*50NT channels was twofold higher than that required to inhibit Cx50 wt channels (520 μM for wt vs. 1.2 mM for Cx46*50NT). In contrast, the concentration–response curve for inhibition of Cx50*46NT channels is further shifted to the right, overlapping with the curve for Cx46 wt channels at concentrations between 300 μM and 1 mM. However, the application of higher concentrations caused a greater reduction in current magnitude in Cx50*46NT-expressing oocytes compared with those expressing Cx46. These results indicate that the amino terminus is an important determinant of the different sensitivities of Cx50 and Cx46 hemichannels to inhibition by BQ^+, although the segregation of inhibition produced by BQ^+ is not entirely restricted to the amino terminus.

DISCUSSION

Quinine has been shown to inhibit GJ channel currents in a connexin subtype–selective manner. Junctional channels strongly inhibited by quinine include those formed by Cx50 and Cx36 at concentrations between 30 to 300 μM. Cx26, Cx32, Cx40, and Cx43 showed poor inhibition (Srinivas et al., 2001). The pH dependence of inhibition and the sidedness of BQ^+'s action suggested that these drugs produce their effect by gaining access to the channel-binding site via the cytoplasm. Whether the binding site is in the pore or in an exposed intracellular domain was not assessed, and the mechanism of action could not be further explored because of the difficulty in obtaining stable recordings of single GJ channels between any given cell pair. In addition, the single-channel data suggested that quinine may alter GJ channel gating, but open-channel block could not be ruled out.

Undocked hemichannels and GJ channels show the same specificity for BQ^+

Conserved gating and permeability characteristics of GJ channels and their corresponding hemichannels suggest that the structures of docked and undocked hemichannels are very similar (Trexler et al., 2000; Valiunas

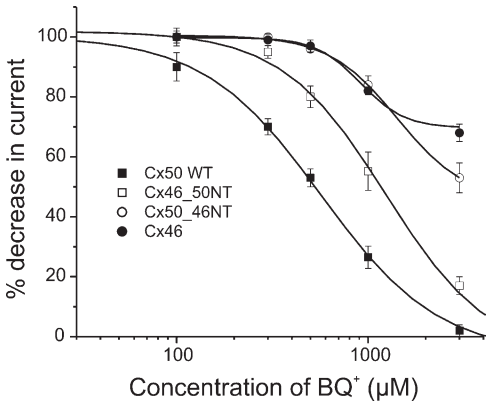

Figure 9. The NT contributes to the difference in the sensitivity of Cx46 and Cx50 hemichannels to BQ^+. Concentration–response curves for the inhibition of macroscopic hemichannel currents in oocytes expressing Cx50 wt (closed squares), Cx46 wt (closed circles), Cx46*50NT (open squares), and Cx50*46NT (open circles). Oocytes were voltage clamped at −70 mV. Current magnitude in oocytes expressing Cx46*50NT, in which Cx46 NT sequence was replaced with that of Cx50, was substantially reduced by 0.5 mM to 3 mM BQ^+. The reciprocal chimera, Cx50*46NT, was similar to Cx46 in being largely insensitive to BQ^+ at all concentrations except 3 mM. Each point represents the mean ± SEM from four different oocytes

and Weingart, 2000; Beahm and Hall, 2002; Kreuzberg et al., 2005; Srinivas et al., 2005). Docking, however, could produce sufficient changes in structure that could render an inhibitor effective in one configuration and not the other. Thus, we tested whether BQ^+ inhibited Cx50 hemichannels, like their Cx50 GJ channel counterparts. Cx50 hemichannels, indeed, were inhibited by BQ^+ at comparable concentrations that inhibited Cx50 GJ channels. In addition, BQ^+ exhibited the same Cx specificity in hemichannels as in GJ channels. We used Cx46, a close homologue of Cx50, and showed that both Cx46 GJ channels and hemichannels were insensitive to BQ^+. Thus, hemichannels, whether in their docked or undocked configurations, maintain the essential structural components that constitute the BQ^+-binding site.

BQ^+ binds in the pore

Excision of patches containing single Cx50 hemichannels in inside-out and outside-out configurations allowed us to examine sidedness of BQ^+ action. We found that BQ^+ added to either side could effectively inhibit Cx50 hemichannels. Moreover, inhibition by BQ^+ was voltage dependent, such that inhibition increased when the polarity of voltage favored entry of BQ^+ into the pore. Thus, hyperpolarization increased inhibition when BQ^+ was added to the extracellular side, and conversely, depolarization increased inhibition when it was added to the cytoplasmic side. These data support a binding site for BQ^+ within the Cx channel pore and are consistent with the effects observed in Cx50 GJ channels, which showed inhibition only when BQ^+ was applied intracellularly (Srinivas et al., 2001). Analysis of voltage dependence of inhibition is suggestive of a binding site toward the cytoplasmic end. Our chimeric data, in which we exchanged NT domains of Cx50 and Cx46, showed that inhibition by BQ^+ segregated with the NT domain of Cx50, supporting NT as a potential binding site.

With a binding site in the pore, why would channel block not occur? The simple explanation may be that Cx channels are rather large. In the recently published crystal structure of the Cx26 GJ channel, the pore is described as a funnel, starting about midway in the TM span and extending extracellularly (Maeda et al., 2009; Fig. 10). The NT domains contribute to the cytoplasmic vestibule of the pore . This domain loops back into the membrane but converges to a narrow point at its terminal end, forming the entrance to the pore funnel. After NT toward the cytoplasm and onto the TM2 domain, the pore flares considerably, forming a wide cytoplasmic vestibule. Estimated diameters are ~12–14 Å at its narrowest at the entrance of the pore funnel and ~40 Å at the wide cytoplasmic entrance. The dimensions of BQ^+ (mol wt, 400) are 11.5 × 9.2 Å. If BQ^+ binds to the NT domain, as suggested by our chimeric data, residence within the wide vestibule of the pore would make block, whether steric or electrostatic, unlikely even upon binding two BQ^+ molecules. The application of the substituted cysteine accessibility method to single Cx50 and Cx46 hemichannels has shown that modification of pore residues with charged methanethiosulphonate reagents, MTSET or MTSES, alters unitary conductance but does not cause conduction block, even when six subunits are modified (Kronengold et al., 2003; Verselis et al., 2009). Even modification with a large thiol reagent such as MTS-biotin failed to completely block the hemichannel. Conductance changes required that multiple subunits be modified, as little or no change was evident with only one or two subunits modified. Moreover, those residues

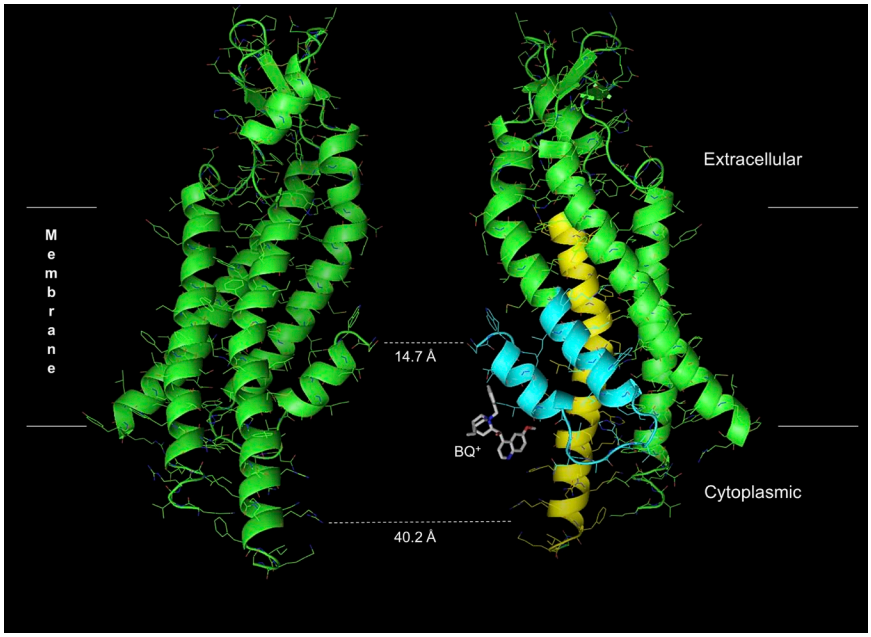

Figure 10. Illustration of BQ^+ in the cytoplasmic vestibule of the connexin pore. The crystal structure of Cx26 by Maeda et al., (2009) with BQ^+ placed in the wide vestibule constituted by NT domain, as suggested by the chimeric data, is shown. For clarity, only two of the six connexin subunits are illustrated. The NT and the TM2 domains of one of the subunits are shown in cyan and yellow, respectively. The pore funnel is formed by the NT TM1 and E1 domains, with the narrowest part ~14.7 Å formed by amino-terminal ends of NT. Pore diameter at the cytoplasmic vestibule, constituted by the NT extending into TM2, widens to ~40 Å. BQ^+ (white) is shown in this wide vestibule. The placement and orientation of BQ^+ is arbitrary. The image was prepared using PyMOL (http://www.pymol.org).

were located in the putative narrower pore funnel region (TM1 and E1), where modifications are more likely to affect ionic flux.

BQ^+ appears to act by modulating an intrinsic gating mechanism, termed loop gating

Using conditions under which native closing events are typically rare, i.e., submicromolar Ca^{2+} and membrane voltages less than or equal to −70 mV, the application of BQ^+ to single Cx50 hemichannels produced frequent closing events. The events observed in the presence of BQ^+ were indistinguishable from those seen with membrane hyperpolarization and, in the presence of low pH, elevated concentrations of divalent cations, all conditions that promote loop gating (one of two mechanisms that gate GJ channels and hemichannels; Trexler et al., 1999; Bukauskas and Verselis, 2004; Srinivas et al., 2005). Loop-gating gating transitions consist of a series of brief substates en route to full opening/closure; a full transition can take 20–50 msec to complete. When closed, the current typically shows frequent noisy current fluctuations or "chirps" from the baseline that likely represent opening attempts comprised of brief sojourns to some of the transient substates that characterize this gating process (Trexler et al., 1996, 1999; Bukauskas and Verselis, 2004; Verselis and Srinivas, 2008). The expectation for hemichannel block would be to observe rapid blocking events that bear no resemblance to these distinctive native loop-gating events. However, direct evidence that the modulation of loop gating is the primary mechanism by which BQ^+ produces its effects is lacking in that it requires independent alteration of loop gating and concomitant examination of changes in inhibition produced by BQ^+. Thus, direct confirmation awaits elucidation of the molecular details of the structural rearrangements underlying loop gating. Although there is evidence that movement of residues in the first extracellular loop, E1, are important for loop gating (Tang et al., 2009; Verselis et al., 2009), the mechanism of closure of the loop gate remains largely unknown and could involve transduction via E1 to TM1 to NT (Verselis et al., 2009). Interactions between NT residues at the entrance to the pore funnel as well as interactions of NT residues with the adjacent TM1 domain have been proposed both to stabilize the pore and to mediate gating by regulating opening and closing of the funnel entrance (Maeda et al., 2009). Thus, binding of BQ^+ to the NT domain could affect the energetics of these interactions and promote gating.

Analysis of dwell times suggests a complex mechanism of action

Examination of dwell times of single Cx50 hemichannels in the presence of BQ^+ showed apparent concentration-dependent changes both in open times and closed times. The application of BQ^+ induced frequent gating transitions, thereby shortening the normally long open times characteristic of Cx50 hemichannels under the recording conditions used (i.e., low extracellular Ca^{2+}). This concentration-dependent decrease in open times can be interpreted in a straightforward manner as binding of BQ^+ to the open state, thereby promoting closure. As we have indicated, quantitative analysis of closed times was problematic, but it is evident that higher BQ^+ concentrations produce longer closed times and less chirping (Figs. 3 and 8). These characteristics are consistent with those of loop gating examined in the most well-studied hemichannel, Cx46, where longer closed times and reduced chirping are associated with hyperpolarization and/or elevation of the levels of extracellular divalent cations, conditions that promote closure of the loop gate. These increased channel closed times with BQ^+ concentration indicates that the action of BQ^+ is more complex than a simple increase in hemichannel closing rate, suggesting that BQ^+ binds to a nonconducting state of the hemichannel, as well. How is this possible when BQ^+ binds in the pore and is effective from either side of the hemichannel? A likely explanation is the presence of multiple binding sites for BQ^+, with closed times depending on the number of bound BQ^+ molecules. This is certainly plausible given the hexameric nature of Cx hemichannels and is supported by the fitting of the fractional inhibition data at different concentrations to the Hill equation, which indicated the presence of at least two binding sites for BQ^+. Thus, it is possible that occupancy of one binding site by BQ^+ closes the hemichannel, and binding to the second site within the channel promotes residence in another, more stable closed state. Although we did not show multiple, discrete closed times in our analysis of closed durations when BQ^+ was applied from the outside, the analysis was compromised by the inherent noisy fluctuations in the closed-state current, which required that we ignore many of the brief subthreshold events. The fluctuations were generally not decipherable, as discrete steps and their varied amplitudes and high frequency imposed considerable difficulties in reaching criteria for inclusion or exclusion. Thus, this inherent difficulty in analysis likely masks a complex distribution of closed times induced by BQ^+. We did see a broader distribution of closed times in the presence of BQ^+, perhaps as a result of a mixing of closed durations that can be fit reasonably well by a single exponential.

When applied to the cytoplasmic side, the fluctuations were less frequent and the closing events appeared more stable (Fig. 8). We could not obtain a sufficient number of stable inside-out patches for extensive analysis, but this tendency is clearly evident in the recordings shown in Fig. 8 as well as in the ramp data in Fig. 7. A possible explanation is that a key binding site for BQ^+ is cytoplasmic to the site at which the loop gate closes the hemichannel. Thus, when applied from the cytoplasmic

side, BQ^+ has access to this site in open and closed conformations, thereby exhibiting a stabilizing effect on closures. When applied from the outside, closure of the gate would block access to this binding site, which should promote unbinding and reopening. Increasing the concentration of BQ^+ could increase closed durations if the incidence of multiple binding is promoted before closure as occupancy of the drug within the pore increases, explaining, in part, the more frequent chirping in current and the lower number of stable closings with BQ^+ applied from the outside compared with that from the inside.

Increase of macroscopic currents by BQ^+

In addition to inhibition of Cx50 hemichannels, we observed a secondary effect of BQ^+ on macroscopic currents. At lower concentrations that produced partial inhibition, the remaining current increased in the continued presence of BQ^+. After BQ^+ was washed out, the currents were larger than those before BQ^+. This increase is similar to the effects of quinine, which is known to potentiate hemichannel currents in oocytes expressing certain connexins (e.g., Cx35) (Malchow et al., 1994a,b; White et al., 1999). Such a potentiation was not observed in excised patch recordings of single Cx50 hemichannels, suggesting that the effects observed macroscopically resulted from recruitment of hemichannels to the membrane. The increase was variable among oocytes but was present in all oocytes. A second application of BQ^+ in rapid succession did not show an increase, suggesting that there is some readily available pool that can either be inserted or activated. We did not examine this further as it may be specific to oocytes, which show active insertion and removal of vesicles carrying Cxs and other proteins (Zampighi et al., 1999).

In summary, this is the first examination of mechanism of action of a Cx-specific inhibitor in excised patches. Our study demonstrates the usefulness of hemichannel preparation to study drug actions on Cx channels. The quinine derivatives appear to be modifiers of gating rather than pore blockers of connexin channels.

This work was supported by National Institutes of Health grants (EY013869 and NS064417 to M. Srinivas and GM54179 to V.K. Verselis).

Kenton J. Swartz served as editor.

Submitted: 14 June 2011
Accepted: 29 November 2011

REFERENCES

Beahm, D.L., and J.E. Hall. 2002. Hemichannel and junctional properties of connexin 50. *Biophys. J.* 82:2016–2031. http://dx.doi.org/10.1016/S0006-3495(02)75550-1

Bukauskas, F.F., and V.K. Verselis. 2004. Gap junction channel gating. *Biochim. Biophys. Acta.* 1662:42–60. http://dx.doi.org/10.1016/j.bbamem.2004.01.008

Cruikshank, S.J., M. Hopperstad, M. Younger, B.W. Connors, D.C. Spray, and M. Srinivas. 2004. Potent block of Cx36 and Cx50 gap junction channels by mefloquine. *Proc. Natl. Acad. Sci. USA.* 101:12364–12369. http://dx.doi.org/10.1073/pnas.0402044101

DeRosa, A.M., C.H. Xia, X. Gong, and T.W. White. 2007. The cataract-inducing S50P mutation in Cx50 dominantly alters the channel gating of wild-type lens connexins. *J. Cell Sci.* 120:4107–4116. http://dx.doi.org/10.1242/jcs.012237

Dong, L., X. Liu, H. Li, B.M. Vertel, and L. Ebihara. 2006. Role of the N-terminus in permeability of chicken connexin45.6 gap junctional channels. *J. Physiol.* 576:787–799. http://dx.doi.org/10.1113/jphysiol.2006.113837

Gerido, D.A., A.M. DeRosa, G. Richard, and T.W. White. 2007. Aberrant hemichannel properties of Cx26 mutations causing skin disease and deafness. *Am. J. Physiol. Cell Physiol.* 293:C337–C345. http://dx.doi.org/10.1152/ajpcell.00626.2006

Kreuzberg, M.M., G. Söhl, J.S. Kim, V.K. Verselis, K. Willecke, and F.F. Bukauskas. 2005. Functional properties of mouse connexin30.2 expressed in the conduction system of the heart. *Circ. Res.* 96:1169–1177. http://dx.doi.org/10.1161/01.RES.0000169271.33675.05

Kronengold, J., E.B. Trexler, F.F. Bukauskas, T.A. Bargiello, and V.K. Verselis. 2003. Pore-lining residues identified by single channel SCAM studies in Cx46 hemichannels. *Cell Commun. Adhes.* 10:193–199.

Maeda, S., S. Nakagawa, M. Suga, E. Yamashita, A. Oshima, Y. Fujiyoshi, and T. Tsukihara. 2009. Structure of the connexin 26 gap junction channel at 3.5 Å resolution. *Nature.* 458:597–602. http://dx.doi.org/10.1038/nature07869

Malchow, R.P., H. Qian, L.M. Haugh-Scheidt, and H. Ripps. 1994a. The effects of quinine and quinidine on isolated retinal horizontal cells. *Biol. Bull.* 187:262–263.

Malchow, R.P., H. Qian, and H. Ripps. 1994b. A novel action of quinine and quinidine on the membrane conductance of neurons from the vertebrate retina. *J. Gen. Physiol.* 104:1039–1055. http://dx.doi.org/10.1085/jgp.104.6.1039

Mese, G., V. Valiunas, P.R. Brink, and T.W. White. 2008. Connexin26 deafness associated mutations show altered permeability to large cationic molecules. *Am. J. Physiol. Cell Physiol.* 295:C966–C974. http://dx.doi.org/10.1152/ajpcell.00008.2008

Minogue, P.J., J.J. Tong, A. Arora, I. Russell-Eggitt, D.M. Hunt, A.T. Moore, L. Ebihara, E.C. Beyer, and V.M. Berthoud. 2009. A mutant connexin50 with enhanced hemichannel function leads to cell death. *Invest. Ophthalmol. Vis. Sci.* 50:5837–5845. http://dx.doi.org/10.1167/iovs.09-3759

Oh, S., J.B. Rubin, M.V. Bennett, V.K. Verselis, and T.A. Bargiello. 1999. Molecular determinants of electrical rectification of single channel conductance in gap junctions formed by connexins 26 and 32. *J. Gen. Physiol.* 114:339–364. http://dx.doi.org/10.1085/jgp.114.3.339

Pfenniger, A., A. Wohlwend, and B.R. Kwak. 2011. Mutations in connexin genes and disease. *Eur. J. Clin. Invest.* 41:103–116. http://dx.doi.org/10.1111/j.1365-2362.2010.02378.x

Purnick, P.E., D.C. Benjamin, V.K. Verselis, T.A. Bargiello, and T.L. Dowd. 2000. Structure of the amino terminus of a gap junction protein. *Arch. Biochem. Biophys.* 381:181–190. http://dx.doi.org/10.1006/abbi.2000.1989

Sánchez, H.A., G. Mese, M. Srinivas, T.W. White, and V.K. Verselis. 2010. Differentially altered Ca^{2+} regulation and Ca^{2+} permeability in Cx26 hemichannels formed by the A40V and G45E mutations that cause keratitis ichthyosis deafness syndrome. *J. Gen. Physiol.* 136:47–62. http://dx.doi.org/10.1085/jgp.201010433

Srinivas, M., M.G. Hopperstad, and D.C. Spray. 2001. Quinine blocks specific gap junction channel subtypes. *Proc. Natl. Acad. Sci. USA.* 98:10942–10947. http://dx.doi.org/10.1073/pnas.191206198

Srinivas, M., J. Kronengold, F.F. Bukauskas, T.A. Bargiello, and V.K. Verselis. 2005. Correlative studies of gating in Cx46 and Cx50 hemichannels and gap junction channels. *Biophys. J.* 88:1725–1739. http://dx.doi.org/10.1529/biophysj.104.054023

Srinivas, M., D.P. Calderon, J. Kronengold, and V.K. Verselis. 2006. Regulation of connexin hemichannels by monovalent cations. *J. Gen. Physiol.* 127:67–75. http://dx.doi.org/10.1085/jgp.200509397

Tang, Q., T.L. Dowd, V.K. Verselis, and T.A. Bargiello. 2009. Conformational changes in a pore-forming region underlie voltage-dependent "loop gating" of an unapposed connexin hemichannel. *J. Gen. Physiol.* 133:555–570. http://dx.doi.org/10.1085/jgp.200910207

Trexler, E.B., M.V. Bennett, T.A. Bargiello, and V.K. Verselis. 1996. Voltage gating and permeation in a gap junction hemichannel. *Proc. Natl. Acad. Sci. USA.* 93:5836–5841. http://dx.doi.org/10.1073/pnas.93.12.5836

Trexler, E.B., F.F. Bukauskas, M.V. Bennett, T.A. Bargiello, and V.K. Verselis. 1999. Rapid and direct effects of pH on connexins revealed by the connexin46 hemichannel preparation. *J. Gen. Physiol.* 113:721–742. http://dx.doi.org/10.1085/jgp.113.5.721

Trexler, E.B., F.F. Bukauskas, J. Kronengold, T.A. Bargiello, and V.K. Verselis. 2000. The first extracellular loop domain is a major determinant of charge selectivity in connexin46 channels. *Biophys. J.* 79:3036–3051. http://dx.doi.org/10.1016/S0006-3495(00)76539-8

Valiunas, V., and R. Weingart. 2000. Electrical properties of gap junction hemichannels identified in transfected HeLa cells. *Pflugers Arch.* 440:366–379. http://dx.doi.org/10.1007/s004240000294

Verselis, V.K., and M. Srinivas. 2008. Divalent cations regulate connexin hemichannels by modulating intrinsic voltage-dependent gating. *J. Gen. Physiol.* 132:315–327. http://dx.doi.org/10.1085/jgp.200810029

Verselis, V.K., C.S. Ginter, and T.A. Bargiello. 1994. Opposite voltage gating polarities of two closely related connexins. *Nature.* 368:348–351. http://dx.doi.org/10.1038/368348a0

Verselis, V.K., M.P. Trelles, C. Rubinos, T.A. Bargiello, and M. Srinivas. 2009. Loop gating of connexin hemichannels involves movement of pore-lining residues in the first extracellular loop domain. *J. Biol. Chem.* 284:4484–4493. http://dx.doi.org/10.1074/jbc.M807430200

White, T.W., M.R. Deans, J. O'Brien, M.R. Al-Ubaidi, D.A. Goodenough, H. Ripps, and R. Bruzzone. 1999. Functional characteristics of skate connexin35, a member of the gamma subfamily of connexins expressed in the vertebrate retina. *Eur. J. Neurosci.* 11:1883–1890. http://dx.doi.org/10.1046/j.1460-9568.1999.00607.x

Willecke, K., J. Eiberger, J. Degen, D. Eckardt, A. Romualdi, M. Güldenagel, U. Deutsch, and G. Söhl. 2002. Structural and functional diversity of connexin genes in the mouse and human genome. *Biol. Chem.* 383:725–737. http://dx.doi.org/10.1515/BC.2002.076

Woodhull, A.M. 1973. Ionic blockage of sodium channels in nerve. *J. Gen. Physiol.* 61:687–708. http://dx.doi.org/10.1085/jgp.61.6.687

Zampighi, G.A., D.D. Loo, M. Kreman, S. Eskandari, and E.M. Wright. 1999. Functional and morphological correlates of connexin50 expressed in *Xenopus laevis* oocytes. *J. Gen. Physiol.* 113:507–524. http://dx.doi.org/10.1085/jgp.113.4.507

Zoidl, G., and R. Dermietzel. 2010. Gap junctions in inherited human disease. *Pflugers Arch.* 460:451–466. http://dx.doi.org/10.1007/s00424-010-0789-1